

Perspective

Liquid-phase TEM study of electrochemical reactions at multiple interfaces

Honglu Hu,¹ Ruijie Yang,² and Zhiyuan Zeng^{1,3,*}¹Department of Materials Science and Engineering and State Key Laboratory of Marine Pollution, City University of Hong Kong, Hong Kong 999077, People's Republic of China²Department of Chemical and Petroleum Engineering, University of Calgary, Calgary, AB T2N 1N4, Canada³Shenzhen Research Institute, City University of Hong Kong, Shenzhen 518057, People's Republic of China

*Correspondence: zhiyzeng@cityu.edu.hk

<https://doi.org/10.1016/j.matt.2024.11.033>

PROGRESS AND POTENTIAL The evolution of liquid-phase transmission electron microscopy (LP-TEM) has marked a significant leap in the study of materials science, particularly within electrochemical energy storage and conversion, by allowing real-time observation of reactions at electrode-electrolyte interfaces. Early methods have progressed to today's sophisticated systems capable of capturing atomic-level transformations, and while challenges such as the need for higher resolution and controlled environments persist, the future of LP-TEM is promising, with the integration of artificial intelligence and advanced imaging techniques set to enhance data collection and analysis, potentially revolutionizing our understanding and development of energy materials.

SUMMARY

The energy landscape is evolving with a focus on sustainable energy storage and conversion, driven by advancements in battery and electrocatalytic systems. Traditional methods have struggled to capture real-time electrochemical reactions, necessitating more nuanced approaches. Liquid-phase transmission electron microscopy (LP-TEM) has emerged as a pivotal tool, enabling *in situ* observation of dynamic processes at the electrode-electrolyte interface. Historical advancements laid the structural groundwork, while recent innovations have significantly enhanced resolution and control in liquid environments. Herein, we provide an overview of the historical development and present state of LP-TEM in the context of electrochemical energy storage and conversion. Additionally, we outline future research directions, focusing on the potential of integrating LP-TEM with *in situ* experimental techniques and algorithm-assisted image analysis to further enhance the understanding of electrochemical mechanisms at the atomic level.

INTRODUCTION

The energy sector is evolving, with a focus on developing sustainable and efficient energy storage and conversion systems. The performance of battery and electrocatalytic systems is critically dependent on the electrochemical reactions occurring at the electrode-electrolyte interfaces.¹ For batteries, the challenge is understanding the formation and evolution of the solid-electrolyte interphase (SEI), which is crucial for performance and stability.² SEI forms from electrolyte decomposition and passivates the electrode, but uncontrolled growth leads to capacity loss and increased impedance. Dendrite growth in metal-based batteries is another critical issue, as it can cause short circuits and safety risks.³ Additionally, ion transport through electrolytes and across interfaces, especially in high-energy-density systems like lithium-sulfur (Li-S) and solid-state batteries, remains poorly understood.⁴ Key processes like ion solvation, desolvation, and

interfacial charge transfer are difficult to capture in real time with conventional methods. In electrocatalysis, the core challenges include identifying active sites and understanding how catalysts dynamically restructure during reactions.⁵ The role of adsorbed intermediates, such as oxygen or hydrogen (in the oxygen evolution reaction [OER] and oxygen reduction reaction [ORR]), and their influence on reaction pathways is not fully clear.⁶ Dynamic surface changes during reactions, including surface reconstruction or shifts in oxidation state, add further complexity, which largely influences catalyst activity, selectivity, and stability.

Traditional methods for studying these processes have been limited by their inability to capture the dynamic behavior of materials as they undergo electrochemical reactions.⁷ Despite ions in the bulk electrolyte forming solvation shells and migrating toward the electrode under an electric field, the formation of the SEI in batteries has been documented.⁸ However, these insights



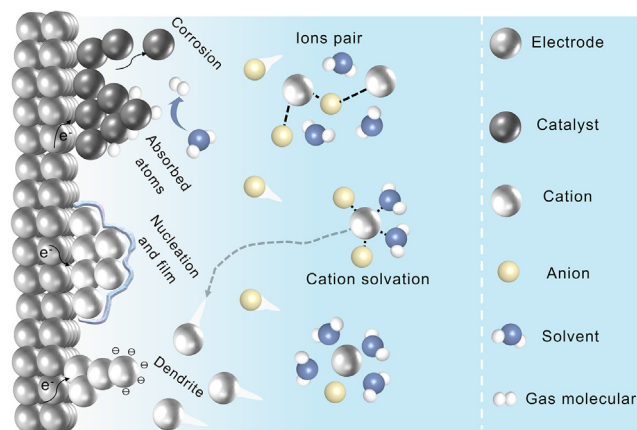


Figure 1. Schematic illustration of reaction processes at the electrochemical interface

A typical solid-liquid electrochemical system can be delineated into three distinct regions: the electrode, the immediate electrode-electrolyte interface, and the bulk electrolyte. The electrode is responsible for charge carrier transport. Within the bulk electrolyte, cations and anions form solvation structures through coordination with solvent molecules, which, under the influence of an electric field, migrate toward the electrode-electrolyte interface. This interface is the site where electrochemical reactions occur. In electrocatalytic reactions, a catalyst facilitates the transformation of reactants by adsorbing them and mediating electron transfer, leading to the progression of the reaction. Concurrently, the catalyst may undergo reconstruction or irreversible degradation during this process. In batteries, the deposition and dissolution of metal ions also take place at this interface. The initial nucleation causes disparities in charge distribution, prompting metals to grow with either smooth or dendritic morphologies. This process is often accompanied by the decomposition of the electrolyte and the formation of an SEI film on the metal surface.

often rely on indirect observations, leaving real-time atomic-level changes elusive.⁹ Critical gaps include how transient species form and interact at the interface, how materials degrade or reconstruct during electrochemical cycling, and how dendritic structures nucleate and grow. The development of liquid-phase transmission electron microscopy (LP-TEM) has provided a significant stride forward in this regard, offering a platform to observe electrochemical processes in their native, solvated environments.¹⁰ This technique allows researchers to directly observe the interactions at the electrode-electrolyte interface, where electrochemical reactions initiate. The study of these reactions has historically been challenging due to the complex and dynamic nature of the electrode interfaces, which are influenced by a variety of factors, including ion pair formation and cation solvation within the electrolyte.¹¹ Figure 1 provides a schematic overview of the well-understood processes at the electrochemical interface, such as ion migration and solvation, but it is in the study of dynamic, real-time changes—such as the formation of transient species, localized degradation, and electrode surface reconstruction—where LP-TEM offers direct observation and where significant gaps in current knowledge remain. Here, we provide a review of LP-TEM study of electrochemical interface reactions, discussing its pioneers and recent advances, analyzing the current challenges and future opportunities.

TECHNOLOGICAL ADVANCES

In the nascent years, the work by Abrams and McBain set the stage for what would become a powerful tool for studying wet samples in 1944 (Figure 2A).¹² Their closed cell for electron microscopy allowed the observation of materials in their natural states. This approach was expanded upon by Parsons, who detailed the structure of wet specimens, illuminating opportunities presented by this methodology (Figure 2B).¹³ The introduction of wet environmental transmission electron microscopy (TEM) further expanded the ability to observe liquid-catalyst reactions directly at the nanoscale, allowing the visualization of dynamic processes such as nucleation and growth.^{14,15} These early advancements in closed-cell electron microscopy provided a critical platform for studying electrochemical interfaces but highlighted the need for more refined setups, particularly in the context of resolving nanoscale processes within liquid environments.

The period from 2009 to 2017 saw significant strides in liquid cell structure within TEM. In 2009, the design of silicon nitride (SiN_x) electron-transparent windows, reduced to a thickness of 25 nm, enabled sub-nanometer imaging resolutions in liquid layers as thin as 200 nm (Figure 2E).¹⁶ This research pioneered the way for visualizing the formation processes of nanoparticles with high clarity. Subsequent developments introduced a liquid flow cell with a resolution of a few nanometers in micrometer-thick liquid water, which facilitated the maintenance of a pristine liquid environment and reduced the impact of the electron beam on the sample (Figure 2F).¹⁷ In 2012, the introduction of graphene-window liquid cells with high electron transmittance marked a significant leap in resolution, particularly for atomic-scale studies of catalytic processes (Figure 2G).¹⁸ The cell operates by confining a thin liquid layer or minute droplets between two graphene sheets, leveraging graphene's thinness to facilitate detailed imaging with atomic resolution. Further developments, such as the heated-flow liquid cell, have expanded the capabilities of LP-TEM by allowing the real-time observation of thermally driven reactions (Figure 2H).¹⁹ In particular, this setup has proved essential for studies of galvanic replacement reactions, where temperature control is critical for influencing reaction pathways and product formation. The incorporation of a syringe pump to introduce precursor solutions under controlled conditions ensures that the liquid environment can be precisely manipulated.

Pioneers improved the resolution and control within LP-TEM, allowing more detailed observations of electrochemical interface reactions. However, challenges still exist in capturing reactions with full spectrum and recording information beyond morphological changes. Early advances primarily focused on overcoming limitations such as spatial resolution and beam-induced artifacts. These efforts concentrated on refining the liquid cell design, ensuring better isolation of the liquid environment from the electron beam and enhancing the imaging quality for observing electrochemical processes in real time. Moreover, the introduction of high-angle annular dark-field scanning TEM (HAADF-STEM) in liquid-phase settings significantly enhanced contrast and spatial resolution, making it possible to resolve atomic-scale features of electrode materials and their dynamic transformations.²⁴

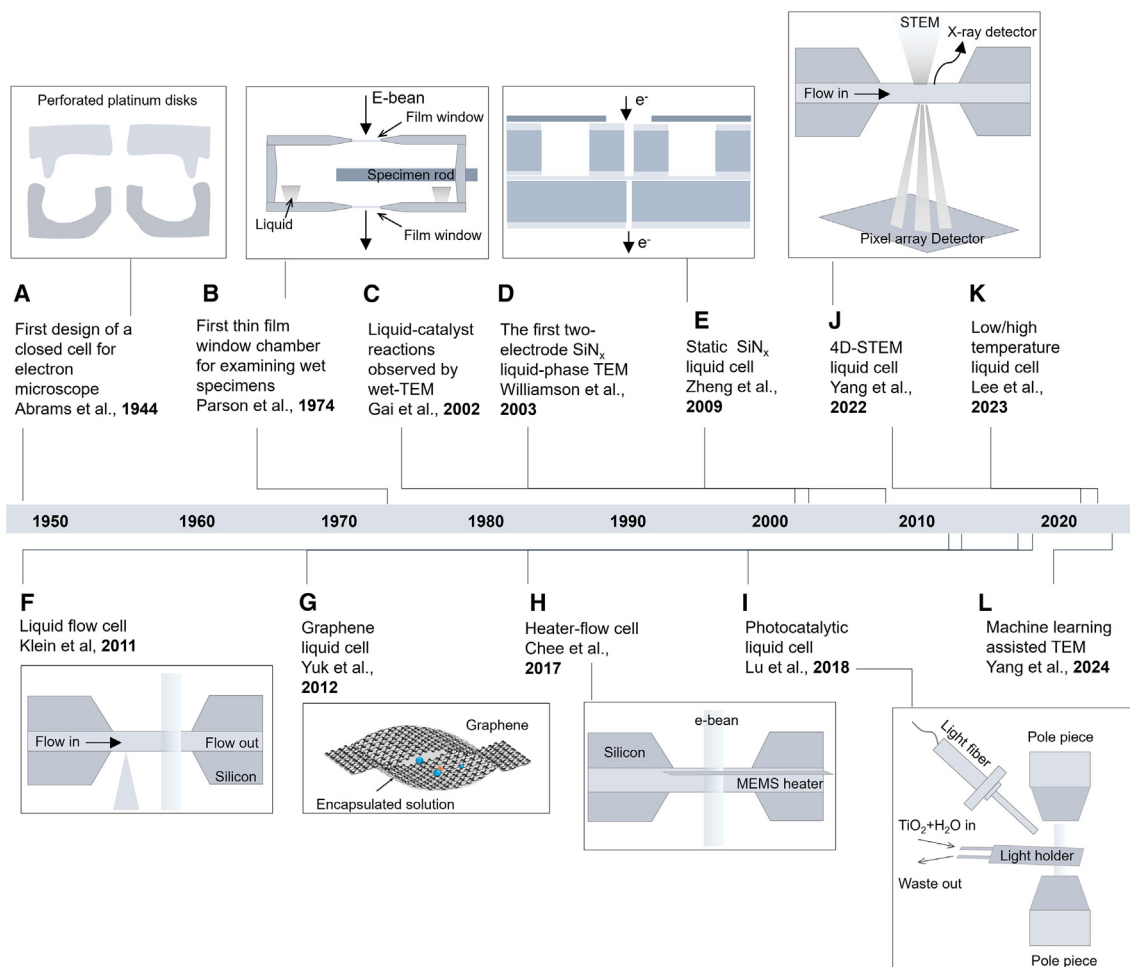


Figure 2. A brief history of design for LP-TEM

- (A) Schematic representation of the first closed cell.¹²
 (B) Schematic representation of the thin window chamber.¹³
 (C) Brief introduction to wet-TEM.¹⁴
 (D) Brief introduction to the first two-electrode SiN_x liquid-phase TEM.¹⁵
 (E) Schematic representation of the first static SiN_x liquid cell.¹⁶
 (F) Schematic representation of the liquid flow cell.¹⁷
 (G) Schematic representation of the graphene liquid cell.¹⁸
 (H) Schematic representation of the heater-flow liquid cell.¹⁹
 (I) Schematic representation of the photocatalytic liquid cell.²⁰
 (J) Schematic representation of the 4D-STEM liquid cell.²¹
 (K) Brief introduction to low-/high-temperature liquid-phase TEM.²²
 (L) Brief introduction to machine-learning-assisted TEM.²³

More recent works have focused on addressing these challenges and further enhancing the capabilities of LP-TEM, particularly in providing quantitative insights into electrochemical reactions. The study by Lu et al. on photocatalytic hydrogen evolution coupled LP-TEM with an optical fiber to allow a photochemical liquid cell in a genuine water environment under UV illumination (Figure 2I).²⁰ In this setup, LP-TEM was instrumental in capturing the formation and migration of hydrogen bubbles, which helps to understand photocatalytic processes at the interface of solid catalysts and liquid environments under light exposure. The combination of 4D-STEM and LP-TEM offered insights

into how substrate orientation influences the growth and nucleation of metallic layers from atomic-scale changes (Figure 2J).²¹ In 2023, Lee et al. explored temperature-dependent nanochemistry and growth kinetics, underlining the importance of environmental factors in material science.²² Their LP-TEM experiments meticulously tracked the temperature-induced changes in the growth rates and morphologies of nanocrystals, providing critical data on how thermal fluctuations impact reaction kinetics and material stability in liquid environments. The work by Yang et al. discusses the application of *operando* LP-TEM in conjunction with machine-learning techniques to study the dynamic

evolution of Cu nanowires during the electrochemical CO₂ reduction reaction (CO₂RR).²³ The use of *operando* LP-TEM provided real-time imaging of the reduction and partial reoxidation processes of the Cu nanograins, while machine-learning-assisted 4D-STEM analysis helped in deciphering the complex grain boundaries within the nanograins. Moreover, the use of electron energy-loss spectroscopy (EELS) in conjunction with LP-TEM has revealed the oxidation states of Cu during CO₂RR, showcasing the technique's capability to combine morphological and chemical analysis. These recent innovations have pushed the boundaries of what can be observed within LP-TEM, providing a more comprehensive view of electrochemical interfaces.

RECENT INVESTIGATIONS

Battery chemistries have made significant strides, yet the complexity of interface reactions during electrochemical cycling poses challenges that can lead to capacity fade and shortened lifespans.²⁵ Despite the high specific capacity that battery materials offer, their electrochemical cycling can result in a cascade of structural and compositional changes that are not fully understood.²⁶ The ability to monitor and interpret these changes in real time is essential for developing strategies to mitigate degradation and enhance battery performance.

The *operando* electrochemical LP-TEM technique has advanced our understanding of Li dendrite formation, growth, and dissolution, particularly through early pioneering studies. These investigations demonstrated that dendrite growth is highly localized, driven by anisotropic nucleation sites influenced by non-uniform electric fields and surface energy variations, challenging the idea of uniform deposition across the electrode surface.²⁷ Additionally, these studies revealed that the SEI is not static but undergoes continuous restructuring, leading to progressive electrolyte consumption and the formation of "dead Li," which significantly impacts cycle life and capacity retention.²⁸ Observations further indicated that, even at low current densities, dendrites form persistently, highlighting the limitations of SEI passivation in preventing growth.²⁹ Moreover, nanoscale features like lithium fluoride (LiF) sheets were found to form on the electrode surface, offering some stabilization but raising concerns about irregular Li deposition and SEI degradation over time.²⁴

In recent studies, the detailed visualization of Li dendrites has revealed that these structures grow in stages, first via root formation and later by tip extension (Figure 3A).³⁰ The nucleation of dendrites and their subsequent evolution through multiple stages, as captured by LP-TEM, highlights the significant impact of SEI composition and structure on dendrite behavior.^{31,32} Despite the valuable insights from these studies, it is important to note that the liquid cell setup often uses an O-ring rather than indium metal and epoxy to seal the liquid compartments. This design creates a thicker liquid layer, which can reduce spatial resolution of Li dendrites at the nanoscale. This diminished clarity may obscure critical details about early nucleation stages and subtle morphological changes during growth, indicating a need for refinement in the experimental setup. Furthermore, LP-TEM has been applied to the study of cathode-electro-

lyte interphases (CEIs), providing direct insights into the formation and behavior of inorganic components such as LiF nanosheets (Figure 3B).³³ Through real-time visualization within an electrochemical liquid cell, the study meticulously captures the nucleation, growth, merging, and self-healing detachment of LiF. *In situ* LP-TEM observations of LiF nanosheets have shown that their growth is not linear but involves interactions between the electrolyte and the electrode surface, which can lead to both merging and detachment. It is worth noting that the chemical composition analysis, such as selected area electron diffraction, was conducted after removing the electrolyte and drying the cell, which leaves the possibility of alterations in the material that may not accurately reflect its role during the actual electrochemical process.

Real-time LP-TEM studies have revealed that SEI formation is a multi-step process that begins with the nucleation of inorganic nanoparticles, which then coalesce into a mosaic structure (Figure 3C).³⁴ Such detailed observations have shown that the SEI is not static; instead, it is highly dynamic, with continuous restructuring occurring in response to electrochemical conditions. This dynamic nature of the SEI has significant implications for battery performance, as it directly influences ion transport and mechanical stability. Some limitations in the experimental setup could affect the accuracy of the findings. For instance, the use of a platinum (Pt) reference electrode may lead to inaccuracies in voltage measurements, as Pt electrodes cannot maintain a stable potential as precisely as Ag/AgCl electrodes. This could introduce uncertainties in interpreting the potential-dependent behaviors of the SEI in liquid cells. Moreover, although the choice of glassy carbon (GC) as the working electrode avoids the catalytic effects of Pt or Au, which have often been used in previous works, it differs from the copper (Cu) current collectors often used in practical Li metal batteries.

Expanding on the intricate dynamics within Li-O₂ batteries, recent studies have employed LP-TEM to gain insights into the redox mediator-assisted discharge process (Figure 3D).³⁵ Using LP-TEM, the real-time formation and morphological evolution of lithium peroxide (Li₂O₂) was captured, revealing a two-step growth mechanism. The first step involves lateral expansion into disc-like structures, followed by a vertical transformation into toroidal shapes. This detailed visualization confirms the critical role of the redox mediator in facilitating the solution-phase discharge process, where the mediator aids in the solubilization and transport of intermediates, enabling more uniform deposition of Li₂O₂. The proximity of the deposition to the cathode, as well as the diffusion rate of reduced mediators, directly influences the growth kinetics of Li₂O₂ particles. By unraveling this relationship, LP-TEM provides a strategic platform for optimizing redox mediators and cathode designs aimed at enhancing the efficiency and cyclability of Li/O₂ batteries. These insights are not only applicable to Li/O₂ systems but also extend to other high-energy-density devices, including O₂/CO₂-based batteries, where controlling the deposition and morphology of discharge products is critical for performance.⁴¹ In the realm of Li-S batteries, *in situ* LP-TEM has revealed key insights into the formation and suppression of lithium polysulfides (Li-PSs).³⁶ Direct visualization of Li-PS formation and diffusion in liquid electrolytes, a phenomenon notoriously

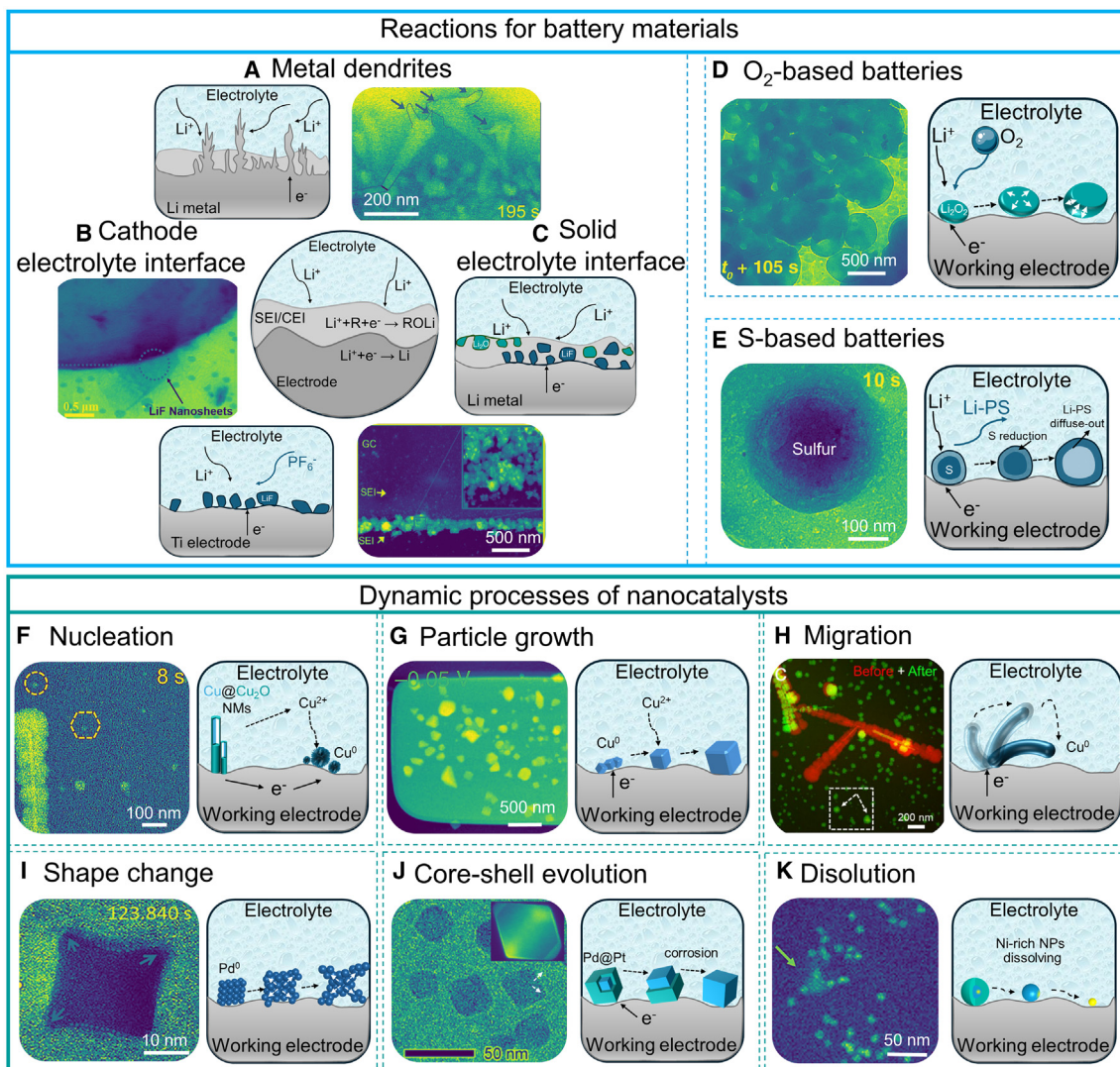


Figure 3. Nanoscale characterization of energy storage and conversion by LP-TEM

- (A) Schematic and ADF-STEM images showing Li dendrites during the growth.³⁰ Copyright 2024, Elsevier.
- (B) Schematic and TEM images of the *in situ*-formed LiF nanosheets in the liquid cell.³³ Copyright 2024, Elsevier.
- (C) Schematic and ADF-STEM images of the formed SEI layer after four cycles.³⁴ Copyright 2023, American Chemical Society.
- (D) Schematic and *in situ* TEM images in Li/O₂ liquid cell during discharge.³⁵ Copyright 2019, American Chemical Society.
- (E) Schematic and TEM images of the morphological evolution of sulfur and dissolved area of Li-PS with lithiation time.³⁶ Copyright 2020, American Chemical Society.
- (F) Schematic and TEM images of initial growth of Cu nanograins from metallic Cu nanowire core.²³ Copyright 2024, American Chemical Society.
- (G) Schematic and STEM images of electrochemical deposition of Cu₂O cubes on the platinum (Pt) electrode at -0.05 V.³⁷ Copyright 2020, Springer Nature.
- (H) Schematic and false-color STEM images (with red indicating before CO₂RR and green indicating after) emphasize the dynamic migration of Cu across different morphologies and locations.²³ Copyright 2024, American Chemical Society.
- (I) Schematic and TEM images of morphological change from center of sides/facets to corners on the surfaces of palladium (Pd).³⁸ Copyright 2018, American Chemical Society.
- (J) Schematic and atomic-resolution STEM images of a Pd@Pt octahedron.³⁹ Copyright 2024, Springer Nature.
- (K) Schematic and HAADF-STEM *in situ* imaging of Ni-rich particle, marked by the arrow, which disappears during cycling.⁴⁰ Copyright 2019, Royal Society of Chemistry.

difficult to observe due to its high solubility and transient nature, was achieved by utilizing the transparency and stability of graphene liquid cells (Figure 3E). Through real-time observation, the technique shows how the ionic liquid stabilizes the sulfur

species in the electrolyte, reducing their mobility and thus limiting the shuttle effect. Building on this, a subsequent study used LP-TEM to probe the dynamic behavior of Li-PS at the atomic scale, uncovering a collective interfacial reaction

pathway.⁴² In contrast to the classical single-molecule reaction pathway, the study revealed how active centers on the electrode surface facilitate the aggregation of soluble Li-PS into dense, droplet-like phases. These dense phases then serve as nucleation sites for the instantaneous deposition of non-equilibrium Li₂S nanocrystals, bypassing the traditional stepwise transformation from Li₂S₂ to Li₂S. The findings underscore the pivotal role of *in situ* LP-TEM in unraveling the complex chemistries within Li/S batteries, offering profound insights into the design of electrolytes to curb the Li-PS shuttle phenomenon.

Nucleation and growth of catalysts are key steps in determining the final morphology and activity of a catalyst. *In situ* LP-TEM enables researchers to witness the initial stages of catalyst formation, where atoms or molecules aggregate to form stable nuclei that then grow into larger structures (Figure 3F).³⁰ Additionally, LP-TEM has provided insights into how the shape and size of the nuclei evolve as a function of reaction parameters, allowing the identification of optimal conditions for controlled growth.³³ This has been particularly valuable in understanding the dynamic evolution of Cu nanowires and cuprous oxide (Cu₂O) particles during CO₂ electrochemical reduction, where the morphological evolution and shape selection are highly dependent on the electrochemical synthesis environment (Figure 3G).^{23,37} This visualization has shed light on the factors that influence nucleation rates and the subsequent growth patterns, such as the choice of precursors, reaction conditions, and the presence of stabilizing agents.

Recent studies underscore the critical role of migration, shape change, and dissolution of catalysts within electrochemical processes, which are paramount for their operational efficacy and durability. The migration of catalyst particles, as observed under an electric field or during chemical reactions, has been captured with striking clarity, demonstrating how these materials can reorient, aggregate, or even fracture (Figure 3H).²³ Such insights are invaluable for the development of robust catalysts tailored for energy conversion and storage technologies, where structural integrity is crucial for long-term performance. Furthermore, shape evolution has been observed in catalysts during electrochemical reactions, where LP-TEM has shown how specific shapes, such as octahedral or cubic nanoparticles, transform into more thermodynamically stable forms. For instance, LP-TEM has revealed that certain shapes with high-index facets are more susceptible to dissolution or degradation under high potential cycling, while enhancing their reactivity and selectivity (Figure 3I).³⁸ The dissolution of catalysts, particularly in the context of core-shell structures, has been illuminated via LP-TEM, where the selective etching or the preferential corrosion of one component can lead to the formation of architectures with enhanced catalytic properties (Figure 3J).³⁹ This technique has shown how the dissolution of the less-noble metal in core-shell nanoparticles can lead to the exposure of catalytically active surfaces, which may enhance activity temporarily but eventually leads to structural collapse if the core is not sufficiently protected. The dynamics of this process have been visualized as it occurs, revealing that the rate and extent of dissolution are strongly influenced by the electro-

chemical potential and the local environment around the particles.

LP-TEM has captured the gradual degradation of Pt-Ni alloy nanoparticles in fuel-cell environments, showing how these catalysts disintegrate over time when subjected to repeated cycling or high potential holds (Figure 3K). Real-time imaging has shown that dissolution often begins at specific sites on the particle, such as edges or grain boundaries, and progresses inward, leading to the loss of catalytic material and eventual particle fragmentation. Furthermore, LP-TEM has revealed that the interaction between the catalyst and its support can influence the rate of dissolution, with weaker interactions leading to faster degradation. This insight is influential for the development of strategies to enhance catalyst stability, such as optimizing the interaction between catalyst particles and their support or modifying the catalyst composition to resist dissolution.

LP-TEM has been instrumental in linking structural changes to performance, showing how the degradation of catalysts over time correlates with a decline in activity. By observing these changes in real time, researchers can now make direct connections between the physical transformations captured by LP-TEM and the electrochemical performance metrics of the catalysts. This has led to the identification of key factors, such as particle size, shape, and composition, that must be controlled to optimize catalyst performance in real systems. Although electrochemical *in situ* LP-TEM is still an emerging technique in the field of batteries and electrocatalytic materials, several advances have already been made (Table 1 provides a summary), which may lead to discoveries and breakthroughs in the field of materials science using LP-TEM in the future.

The growth and etching processes of nanomaterials, particularly in the context of electrocatalysis, involve complex chemical and electrochemical reactions occurring at various interfaces. For instance, LP-TEM has been instrumental in revealing the anisotropic growth of metallic nanostructures, where the growth rate along different crystallographic orientations is influenced by factors such as surface energy and the local chemical environment.⁵⁶ This was observed in the growth of Pt₃Fe nanorods, where small particles attached to the growing nanostructure, followed by elongation in the preferred direction, deviating from classical nucleation models. Similarly, LP-TEM studies on the etching of bimetallic core-shell nanoparticles have demonstrated that dissolution occurs anisotropically, with the core and shell materials exhibiting different dissolution rates depending on their crystallographic orientation and surface energy.⁵⁷ These observations highlight the critical role of real-time imaging in understanding the kinetics of nanomaterial transformation, which is crucial for optimizing their performance in catalytic applications. Moreover, the ability to visualize the transition of nanoparticles into nanosheets, as seen in the formation of two-dimensional transition metal oxide nanosheets, underscores the importance of LP-TEM in studying not only the growth of nanomaterials but also their morphological evolution under operational conditions.⁵⁸ By capturing these processes at the atomic level, LP-TEM enables a deeper understanding of how nanomaterial structures evolve in response to external stimuli, such as biasing or changes in

Table 1. Summary of the recent works on LP-TEM for energy storage and conversion

System	Liquid cell type	Electrolytes in liquid cell	Important findings	Reference
ORR	three-electrode SiN _x cell	0.1 M HClO ₄ in H ₂ O	degradation pathways of Pt-Ni alloy catalysts	Beermann et al. ⁴⁰
Li/O ₂ batteries	two-electrode SiN _x cell	1 M LiClO ₄ in dimethoxyethane	two-step growth mechanism of Li ₂ O ₂	Lee et al. ³⁵
ORR	three-electrode SiN _x cell	0.1 M HClO ₄ in H ₂ O	atomic-level electrochemical Pt dissolution and redeposition	Nagashima et al. ⁴³
Li/Sn batteries	graphene liquid cell	1 M LiPF ₆ in ethylene carbonate/diethyl carbonate	stress effect on Li alloy material	Seo et al. ⁴⁴
Li/Sn batteries	two-electrode SiN _x cell	poly(diallyldimethylammonium chloride) polymer electrolyte	LiF uniformly distributed within the inner SEI layer	Lee et al. ⁴⁵
CO ₂ reduction reaction	three-electrode SiN _x cell	CO ₂ -saturated 0.1 M KHCO ₃ in H ₂ O	shape-selected synthesis of copper oxide cubes	Arán-Ais et al. ³⁷
Li/S batteries	graphene liquid cell	1 M LiTFSI in 1,3-dioxolane/dimethoxyethane	ionic liquid-related Li-polysulfide diffusion	Seo et al. ³⁶
Na metal batteries	two-electrode SiN _x cell	1 M NaPF ₆ in propylene carbonate	Na metal growth on different surface roughness	Zeng et al. ⁴⁶
OER	three-electrode SiN _x cell	0.1 M phosphate buffer	Cu-based clusters formed during first anodic scan	Balaghi et al. ⁴⁷
Li metal batteries	three-electrode SiN _x cell	1 M LiPF ₆ in ethylene carbonate/dimethyl carbonate	fluoride-rich SEI effect on dead Li and electrolyte decomposition	Gong et al. ⁴⁸
Zn metal batteries	three-electrode SiN _x cell	0.1 M ZnSO ₄ in H ₂ O	root-to-tip dissolution for zinc dendrites	Sasaki et al. ³²
Li-ion batteries	three-electrode SiN _x cell	1 M LiClO ₄ in ethylene carbonate/dimethyl carbonate	formation of voids and cracks in LiMn _{1.5} Ni _{0.5} O ₄ cathode	Bhatia et al. ⁴⁹
Li-ion batteries	two-electrode SiN _x cell	1 M LiPF ₆ in propylene carbonate	LiF nanosheet formation on the cathode-electrolyte interphase	Zhang et al. ³³
Li metal batteries	three-electrode SiN _x cell	1 M LiPF ₆ in ethylene carbonate/ethyl methyl carbonate	multi-step process of SEI formation	Dachraoui et al. ³⁴
Hydrogen evolution reaction	three-electrode SiN _x cell	0.1 M NaOH in H ₂ O	Ru-NiPS reconstruction	Fu et al. ⁵⁰
Na metal batteries	three-electrode SiN _x cell	1 M NaPF ₆ in dimethoxyethane/fluoroethylene carbonate	elastic SEI preventing gas evolution	Gong et al. ⁵¹
Na ion batteries	three-electrode SiN _x cell	1 M NaPF ₆ in ethylene carbonate/diethyl carbonate	SEI formation on carbon shell	Hou et al. ⁵²
ORR	three-electrode SiN _x cell	CO ₂ -saturated 0.1 M KHCO ₃ in H ₂ O	structural dynamics during the life cycle of Cu catalysts	Yang et al. ⁵³
Zinc metal batteries	three-electrode SiN _x cell	0.02 M ZnSO ₄ in H ₂ O	epitaxial and stacking growth on Zn deposits	Zeng et al. ³¹
Li/S batteries	two-electrode SiN _x cell	0.1 M Li ₂ S ₆ and 1 M LiTFSI in 1,3-dioxolane/dimethoxyethane	gathering-induced collective charge transfer of Li-PS	Zhou et al. ⁴²
Li metal batteries	three-electrode SiN _x cell	1 M LiPF ₆ in ethylene carbonate/ethyl methyl carbonate	SEI's pivotal role in both Li growth and the dissolution	Dachraoui et al. ³⁰
ORR/hydrogen reduction reaction	three-electrode SiN _x cell	0.1 M HClO ₄ in H ₂ O	electrochemical corrosion of Pd@Pt core-shell electrocatalysts	Shi et al. ³⁹
NO ₃ ⁻ reduction reaction	three-electrode SiN _x cell	0.1 M CuSO ₄ and 0.1 M H ₂ SO ₄ in H ₂ O	electrodeposition of Cu on carbon nanotubes and graphene	Tan et al. ⁵⁴

(Continued on next page)

Table 1. Continued

System	Liquid cell type	Electrolytes in liquid cell	Important findings	Reference
CO ₂ reduction reaction	three-electrode SiN _x cell	CO ₂ -saturated 0.1 M KHCO ₃ in H ₂ O	CO-driven Cu migration and evolution to polycrystalline Cu nanograins	Yang et al. ²³
CO ₂ reduction reaction	polymer liquid cells	CO ₂ -saturated 0.1 M KHCO ₃ in H ₂ O	atomic dynamics of solid-liquid interfaces in liquid	Zhang et al. ⁵⁵

solution composition, thereby linking structural dynamics with electrochemical performance.

Unlike *ex situ* techniques, where conditions can be precisely controlled and measured, the dynamic and *in situ* nature of LP-TEM experiments presents challenges in correlating observed nanoscale transformations with electrochemical performance. To further advance the quantitative assessment of electrochemistry in LP-TEM, a critical area of development lies in the precise quantification and calibration of the external stimuli applied, such as electrical biasing and solution mixing/replacement, which are pivotal in electrochemical reactions. Researchers have begun to integrate calibrated micro-electromechanical systems (MEMSs) within the liquid cells to apply well-defined electrical stimuli, allowing the direct observation of how catalysts respond to controlled potential cycling or biasing.⁵⁹ This setup enables the quantification of key metrics like current density and overpotential, which can be directly linked to the structural changes observed in real time. Additionally, advancements in solution mixing and replacement dynamics within flow reactors have improved the temporal resolution of LP-TEM, allowing more accurate monitoring of rapid chemical reactions.³⁴ For instance, the development of a liquid cell design—the diffusion cell—enhances mass transport dynamics by introducing on-chip bypasses that reduce flow resistance in the system.⁶⁰ This improvement accelerates solution replacement, achieving timescales within seconds. These innovations, coupled with advanced modeling techniques, permit the comparison of *in situ* LP-TEM results with *ex situ* simulated reactors, providing a more comprehensive understanding of how nanoscale processes relate to their macroscopic performance.^{61,62} As these methods evolve, LP-TEM is transitioning from a qualitative tool into a more quantitative and correlative technique, enabling researchers to not only observe but also measure and predict catalyst behavior under realistic operational conditions.

In the context of characterizing electrochemical processes, liquid-phase scanning electron microscopy (LP-SEM) and liquid-phase atomic force microscopy (LP-AFM) have emerged as essential techniques, complementing the capabilities of LP-TEM. Schwager et al. imaged the diffusion behavior of oxygen in Li-air batteries using scanning electrochemical microscopy (SECM) with a microelectrode probe, initially demonstrating the application of LP-SEM in electrochemistry.⁶³ Rong et al. further extended the use of LP-SEM for *in situ* observation of effects of LiNO₃ electrolyte additives on Li dendrite growth kinetics.⁶⁴ However, the spatial resolution of LP-SEM is not as high as that of LP-TEM due to the scattering effect of the liquid layer on the electron beam with low accelerating voltage in SEM. In contrast, LP-SEM, while offering lower spatial resolution, has the advantage of reduced sample damage due to its lower elec-

tron beam energy. This is particularly beneficial for studying samples sensitive to high-energy electron beams, such as organic electrodes and materials with unconventional crystal phases. Unlike electron microscopy techniques that rely on an electron beam, AFM utilizes the local physical interactions between a sharp probe and the sample surface to achieve nanoscale-resolution imaging.⁶⁵ In LP-AFM, the probe is typically submerged in a liquid electrolyte within an open cell for scanning. A laser is focused onto the cantilever through an optical window, with angle adjustments made to correct for refraction at the air-solid-liquid interfaces. By analyzing the cantilever's deflection as the probe approaches, contacts, and withdraws from the surface, the information about the sample's mechanical properties—such as hardness, adhesion, and elasticity—can be obtained.⁶⁶ While LP-AFM operation does not require high vacuum environments, proper sealing of the test cell is essential to prevent liquid leakage and maintain a clear optical path. Moreover, correcting image distortions caused by refraction at the air-solid-liquid boundary is critical to electrochemical LP-AFM measurements. The integration of LP-SEM and LP-AFM, which are not limited to structural analysis but also capable of measuring mechanical stress and surface tension, with LP-TEM can provide multi-angle detection of local reactions and material changes.

CHALLENGES

The integration of LP-TEM in the realms of energy storage and catalysis has broadened our understanding of the dynamic processes occurring within these systems. However, despite the promising prospects of LP-TEM, there are several challenges and concerns that need to be addressed to fully harness its potential.

- (1) A practical challenge with liquid cell TEM experiments for studying electrochemical systems is electron beam damage.⁶⁷ The interaction between the beam and the liquid electrolyte causes radiolysis, leading to the generation of reactive species and gas bubbles that interfere with the observed processes.^{68,69} Radiolysis-induced species, such as hydrated electrons, hydrogen radicals, and hydroxyl radicals, significantly alter the chemistry within the liquid cell, potentially leading to erroneous interpretations of electrochemical reactions. The presence of gas bubbles disrupts the local electrochemical environment, affecting ion transport and reaction kinetics. Additionally, beam-sensitive materials, such as metal-organic frameworks and perovskites used in energy storage, are prone to structural degradation under electron irradiation,

complicating the observation of electrochemical reactions.⁷⁰ Further, these effects obscure the materials' true behavior and introduce artifacts in electrochemical observations. Therefore, it is essential to both understand and suppress these beam-induced effects and to calibrate the experimental stimuli in LP-TEM reactors against *ex situ* setups to ensure accurate interpretation of results. Low-dose imaging methods (i.e., using direct-detection electron-counting cameras) and beam blanking during non-imaging periods are employed to minimize exposure while maintaining image quality.⁷¹ To further assess the electron beam effects, control experiments are crucial. For example, experiments conducted without applying an electrical field (i.e., no cyclic voltammetry) confirm that no observable reactions occur under such conditions.⁷² In the case of Li deposition and bubble formation in a liquid cell, control experiments show that neither precipitation of Li nor bubble formation occurs without an applied electrochemical bias, even under moderate electron current densities ($\sim 5 \times 10^2 \text{ electrons} \cdot \text{\AA}^{-2} \cdot \text{s}^{-1}$).⁷³ These suggest that the electrochemical reactions observed are genuinely driven by the applied electrical field rather than by the electron beam. Beyond these technical fixes, a more comprehensive approach involves the integration of *in situ* spectroscopy and computational modeling to deconvolute the beam effects from the true electrochemical phenomena.⁷⁴ Theoretical simulations of radiolysis in aqueous electrolytes have been used to predict the concentration and lifetime of reactive species, offering a way to correct their impact in post-experiment data analyses.⁷⁵

- (2) Sample preparation is a key challenge in electrochemical LP-TEM. Precisely depositing electrocatalysts or cathode particles onto the working electrode is difficult due to the small microelectrode dimensions. Solutions include nano-pipette deposition, electrophoretic techniques, and SiN_x window functionalization, while lithographic patterning can limit deposition to the working electrode and reduce short-circuit risks.^{76–78} Furthermore, the limited electrolyte volume and electrode proximity in LP-TEM cells lead to non-ideal electrochemical behavior and mass transport, which complicates correlating *in situ* TEM observations with practical battery performance.^{79,80} Spatial limitations also cause localized current density variations, further affecting experimental interpretation. Another problem often faced in experiments is electrolyte selection and compatibility with electrode materials. For example, a high concentration of electrolyte may lead to non-uniform deposition of the electrode material, affecting the repeatability of the results. Optimizing electrode spacing and electrolyte flow helps mitigate these issues. Optimizing the geometry of electrodes is also necessary to ensure uniform current distribution and electric fields, as confined spaces often lead to non-ideal conditions.
- (3) A key challenge in *in situ* TEM is designing a liquid cell that accurately replicates real-world electrochemical conditions. One effective strategy is the use of a three-

electrode system, consisting of a working electrode (WE), a counter electrode (CE), and a reference electrode (RE). This configuration allows precise control over the electrochemical reactions by monitoring potential and current at the WE, facilitating the study of processes like SEI formation, electrode material transformations, and metal ion deposition or dissolution.^{31,34} To sustain the electrochemical environment, the liquid cell must also include an active material source, such as Li metal or a Li-ion intercalation compound (e.g., LiCoO₂), deposited on the CE. This ensures a continuous supply of Li ions, preventing depletion that could skew the reaction dynamics.^{81,82} Maintaining a high-quality electrolyte is another critical issue, as beam damage and electrochemical reactions can degrade or deplete the electrolyte. A flow cell design, with nanochannels integrated into the liquid cell, addresses this by continuously refreshing the electrolyte using a pump-controlled system. This setup not only prevents electrolyte contamination but also allows real-time exchange of electrolytes or reactants.^{17,40}

- (4) Traditional LP-TEM primarily provides insights into the morphological changes of materials, which, while valuable, do not offer a comprehensive characterization of the material's properties.⁵² The lack of additional analytical capabilities, such as chemical state analysis or atomic structure determination, limits the depth of understanding achievable with LP-TEM alone. Further, the vast amount of data generated through LP-TEM requires sophisticated processing and analysis techniques to extract meaningful information.⁵³ Current data-processing methods may not be sufficient to handle the complexity and volume of data, leading to potential inaccuracies or loss of critical details. There is a need for more advanced algorithms and software tools that can efficiently process and analyze LP-TEM data, enabling researchers to derive accurate and actionable insights from their experiments.
- (5) The true power of LP-TEM lies in its ability to observe materials in their native, operational state. However, to fully understand the complex interplay between structure and function, it is necessary to combine LP-TEM with other *in situ* techniques such as X-ray absorption spectroscopy (XAS), 4D-STEM, or EELS. These hybrid approaches can provide a more complete picture of the material's behavior by offering complementary information on electronic and chemical properties.

OPPORTUNITIES

With the advancement of science and technology, emerging techniques such as STEM, 4D-STEM, and atomic electron tomography (AET) have provided deeper insights into the characterization of batteries and catalysts (Figure 4). STEM techniques, by providing subatomic spatial resolution and simultaneous chemical analyses, enable researchers to analyze the critical interfaces and surfaces of individual catalysts, complementing the information provided by other spectroscopic techniques, revealing its surface reconstruction at the atomic level and the

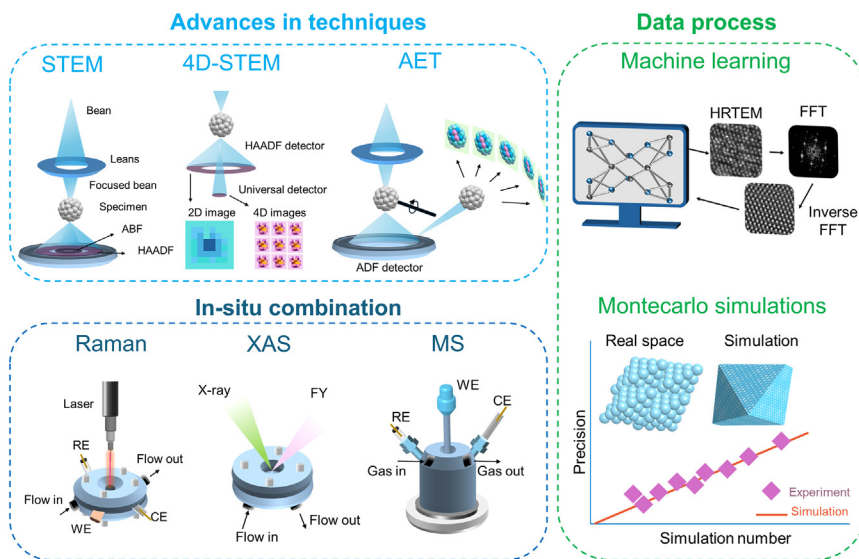


Figure 4. Schematic drawing showing the future development direction of revealing the interface reaction mechanisms by *in situ* LP-TEM

dynamics of the active sites, which are essential for understanding the activity and selectivity of the catalyst.⁸³ 4D-STEM, already implemented in LP-TEM, still presents significant opportunities for further advancement and wider application.⁸⁴ This technique provides a dynamic view of structural evolution under reaction conditions by recording 3D structural information over time. While it has successfully captured real-time changes in catalysts, such as atomic migration and rearrangement, challenges remain in reducing electron beam damage, improving spatial resolution, and advancing data-processing techniques. Addressing these challenges is essential for unlocking its full potential and promoting its broader adoption in catalyst and battery research. AET technique, on the other hand, provides a tool for 3D structural analyses of catalysts by acquiring images from multiple angles and reconstructing the 3D atomic structure.⁸⁵ This technique can reveal the atomic arrangement and defects inside the catalyst, thus providing more precise structural information for catalyst design and optimization.

Data processing is a critical step in the characterization of LP-TEM, which directly affects our understanding of the structure and properties of materials. Traditional LP-TEM techniques, although capable of providing rich structural information, often face challenges when dealing with complex datasets.⁵⁸ Recent advancements in automated image analysis have improved the interpretability of low-dose, noisy LP-TEM images, particularly those capturing dynamic catalytic processes. Methods such as temporal intensity fluctuation analysis and compressive sensing have been applied to reduce noise and enhance image clarity without compromising spatial information. This enables more accurate identification of nanoparticle behavior during catalytic reactions.⁸⁶ The development of advanced techniques such as machine learning and Monte Carlo simulation has provided avenues for in-depth analysis of LP-TEM data. For instance, machine-learning algorithms, specifically U-Net-based convolutional neural networks, have demonstrated robust performance in automatically segmenting and tracking nanoparticle dynamics from high-noise LP-TEM data, even under varying contrast con-

ditions.⁸⁷ By leveraging these algorithms, researchers can efficiently process large-scale LP-TEM video datasets, enabling high-throughput extraction of physical parameters such as particle size, motion trajectories, and interparticle interactions.⁸⁸ Processing LP-TEM images using machine-learning algorithms helps to identify the dynamic changes of nanoparticles from a large amount of data. By training the neural network model, the researchers can automatically detect and analyze the boundaries of the nanoparticles, thus revealing the uneven structural transformations of the nanoparticles in redox environments. Monte Carlo simulations provide another tool for understanding the dynamic behavior of catalysts at the atomic scale.⁶² By simulating the migration and reaction of atoms on a surface, researchers can predict the behavior of catalysts under real reaction conditions. A combination of Monte Carlo simulations and LP-TEM experimental data revealed the transformation paths of nanocrystals in a non-equilibrium state.⁸⁹ This combined experimental and simulation approach, further enhanced by machine-learning-based reconstruction techniques, not only verifies the experimentally observed phenomena but also unveils subtle dynamic features such as curvature-dependent etching and anisotropic interactions.

The development of a variety of *in situ* techniques has provided dimensions to the study of energy materials, especially in liquid-phase conditions, where the application of *in situ* Raman spectroscopy, XAS, and mass spectrometry (MS) techniques have opportunities to enhance the capabilities of conventional LP-TEM for catalyst characterization. Liquid phase *in situ* Raman spectroscopy provides molecular vibrational information, which is essential for understanding the nature of adsorbed species on the catalyst surface and the interactions between the adsorbed species and the catalytic active sites, while XAS detects changes in the electronic structure of the catalyst under reactive conditions, which provides important information for understanding the active center of the catalyst.⁹⁰ Meanwhile, MS plays a complementary role in monitoring the composition of gases generated during reactions in LP-TEM studies with gas evolution, such as SEI formation or electron-beam-induced reactions.^{69,73} However, identification of gases is difficult to characterize directly by the electron beam. The combination of MS techniques allows real-time detection of the composition of gases, providing an effective complementary characterization of gas-generation phenomena that cannot be directly resolved by LP-TEM. The combination of multiple electrochemical *in situ* techniques not only provides structural information on the electrode materials at the atomic scale but also reveals the

dynamic behavior of the electrode materials under actual reaction conditions, providing a more comprehensive understanding of energy material design and optimization.

CONCLUSIONS

The integration of LP-TEM has revolutionized the study of electrochemical processes, providing insights into the dynamic behaviors at the electrode-electrolyte interfaces crucial for energy storage and conversion technologies. This technique has enabled real-time visualization of complex phenomena such as dendrite formation in Li-ion batteries, the growth dynamics of solid-electrolyte interphases, and the morphological evolution of catalysts during reactions. Despite its transformative impact, LP-TEM faces challenges, including the need for enhanced analytical capabilities and sophisticated data-processing methods. Future advancements in combining LP-TEM with complementary *in situ* techniques like XAS and machine-learning algorithms promise to overcome these limitations, offering a more comprehensive understanding of material behaviors. As LP-TEM continues to evolve, it holds the potential to drive breakthroughs in the design and optimization of materials for high-performance batteries and electrocatalysts.

ACKNOWLEDGMENTS

Z.Z. thanks the Young Collaborative Research Grant (project no. C1003-23Y) and the General Research Fund (GRF) (project nos. CityU11308923 and CityU11309824) supports from the Research Grants Council of the Hong Kong Special Administrative Region, China; the Basic Research Project from Shenzhen Science and Technology Innovation Committee in Shenzhen, China (no. JCYJ20210324134012034); the Applied Research Grant of City University of Hong Kong (project no. 9667247); and the Chow Sang Sang Group Research Fund of City University of Hong Kong (project no. 9229123) for the support. Z.Z. is also grateful for funding support from the Seed Collaborative Research Fund Scheme of State Key Laboratory of Marine Pollution, which receives regular research funding from the Innovation and Technology Commission (ITC) of the Hong Kong SAR Government. However, any opinions, findings, conclusions, or recommendations expressed in this publication do not reflect the views of the Hong Kong SAR Government or the ITC.

AUTHOR CONTRIBUTIONS

Supervision and conceptualization, Z.Z.; writing – original draft, Z.Z., H.H., and R.Y.; writing – review & editing, Z.Z.

DECLARATION OF INTERESTS

The authors declare no competing interests.

REFERENCES

- Yang, X., Ni, Y., Lu, Y., Zhang, Q., Hou, J., Yang, G., Liu, X., Xie, W., Yan, Z., Zhao, Q., and Chen, J. (2022). Designing quinone-based anodes with rapid kinetics for rechargeable proton batteries. *Angew. Chem. Int. Ed.* *61*, e202209642. <https://doi.org/10.1002/anie.202209642>.
- Jagger, B., and Pasta, M. (2023). Solid electrolyte interphases in lithium metal batteries. *Joule* *7*, 2228–2244. <https://doi.org/10.1016/j.joule.2023.08.007>.
- Liang, H., Wang, L., Sheng, L., Xu, H., Song, Y., and He, X. (2022). Focus on the electroplating chemistry of Li ions in nonaqueous liquid electrolytes: Toward stable lithium metal batteries. *Electrochem. Energy Rev.* *5*, 23. <https://doi.org/10.1007/s41918-022-00158-2>.
- Li, G. (2021). Regulating mass transport behavior for high-performance lithium metal batteries and fast-charging lithium-ion batteries. *Adv. Energy Mater.* *11*, 2002891. <https://doi.org/10.1002/aenm.202002891>.
- Zhong, H., Zhang, Q., Yu, J., Zhang, X., Wu, C., Ma, Y., An, H., Wang, H., Zhang, J., Wang, X., and Xue, J. (2023). Fundamental understanding of structural reconstruction behaviors in oxygen evolution reaction electrocatalysts. *Adv. Energy Mater.* *13*, 2301391. <https://doi.org/10.1002/aenm.202301391>.
- Liu, X.-M., Cui, X., Dastafkan, K., Wang, H.-F., Tang, C., Zhao, C., Chen, A., He, C., Han, M., and Zhang, Q. (2021). Recent advances in spinel-type electrocatalysts for bifunctional oxygen reduction and oxygen evolution reactions. *J. Energy Chem.* *53*, 290–302. <https://doi.org/10.1016/j.jechem.2020.04.012>.
- Wang, K., Qiu, T., Lin, L., Liu, X.-X., and Sun, X. (2023). A low fraction electrolyte additive as interface stabilizer for Zn electrode in aqueous batteries. *Energy Storage Mater.* *54*, 366–373. <https://doi.org/10.1016/j.ensm.2022.10.029>.
- Kondo, Y., Abe, T., and Yamada, Y. (2022). Kinetics of interfacial ion transfer in lithium-ion batteries: Mechanism understanding and improvement strategies. *ACS Appl. Mater. Interfaces* *14*, 22706–22718. <https://doi.org/10.1021/acsami.1c21683>.
- Yang, R., Mei, L., Lin, Z., Fan, Y., Lim, J., Guo, J., Liu, Y., Shin, H.S., Voiry, D., Lu, Q., et al. (2024). Intercalation in 2D materials and *in situ* studies. *Nat. Rev. Chem* *8*, 410–432. <https://doi.org/10.1038/s41570-024-00605-2>.
- Zheng, H., Lu, X., and He, K. (2022). *In situ* transmission electron microscopy and artificial intelligence enabled data analytics for energy materials. *J. Energy Chem.* *68*, 454–493. <https://doi.org/10.1016/j.jechem.2021.12.001>.
- Liang, P., Hu, H., Dong, Y., Wang, Z., Liu, K., Ding, G., and Cheng, F. (2024). Competitive coordination of ternary anions enabling fast Li-ion desolvation for low-temperature lithium metal batteries. *Adv. Funct. Mater.* *34*, 2309858. <https://doi.org/10.1002/adfm.202309858>.
- Abrams, I.M., and McBain, J.W. (1944). A closed cell for electron microscopy. *J. Appl. Phys.* *15*, 607–609. <https://doi.org/10.1063/1.1707475>.
- Parsons, D.F. (1974). Structure of wet specimens in electron microscopy. *Science* *186*, 407–414. <https://doi.org/10.1126/science.186.4162.407>.
- Gai, P.L. (2002). Development of wet environmental TEM (Wet-ETEM) for *in situ* studies of liquid-catalyst reactions on the nanoscale. *Microsc. Microanal.* *8*, 21–28. <https://doi.org/10.1017/s143192760201005x>.
- Williamson, M.J., Tromp, R.M., Verbeeck, P.M., Hull, R., and Ross, F.M. (2003). Dynamic microscopy of nanoscale cluster growth at the solid-liquid interface. *Nat. Mater.* *2*, 532–536. <https://doi.org/10.1038/nmat944>.
- Zheng, H., Smith, R.K., Jun, Y.-w., Kisielowski, C., Dahmen, U., and Alivisatos, A.P. (2009). Observation of single colloidal platinum nanocrystal growth trajectories. *Science* *324*, 1309–1312. <https://doi.org/10.1126/science.1172104>.
- Klein, K.L., Anderson, I.M., and De Jonge, N. (2011). Transmission electron microscopy with a liquid flow cell. *J. Microsc.* *242*, 117–123. <https://doi.org/10.1111/j.1365-2818.2010.03484.x>.
- Yuk, J.M., Park, J., Ercius, P., Kim, K., Hellebusch, D.J., Crommie, M.F., Lee, J.Y., Zettl, A., and Alivisatos, A.P. (2012). High-resolution em of colloidal nanocrystal growth using graphene liquid cells. *Science* *336*, 61–64. <https://doi.org/10.1126/science.1217654>.
- Chee, S.W., Tan, S.F., Baraissov, Z., Bosman, M., and Mirsaidov, U. (2017). Direct observation of the nanoscale kirkendall effect during galvanic replacement reactions. *Nat. Commun.* *8*, 1224. <https://doi.org/10.1038/s41467-017-01175-2>.
- Lu, Y., Yin, W.-J., Peng, K.-L., Wang, K., Hu, Q., Selloni, A., Chen, F.-R., Liu, L.-M., and Sui, M.-L. (2018). Self-hydrogenated shell promoting photocatalytic H₂ evolution on anatase TiO₂. *Nat. Commun.* *9*, 2752. <https://doi.org/10.1038/s41467-018-05144-1>.

21. Yang, Y., Shao, Y.-T., DiSalvo, F.J., Muller, D.A., and Abruña, H.D. (2022). Metal monolayers on command: Underpotential deposition at nanocrystal surfaces: A quantitative *operando* electrochemical transmission electron microscopy study. *ACS Energy Lett.* **7**, 1292–1297. <https://doi.org/10.1021/acsenergylett.2c00209>.
22. Lee, S., Schneider, N.M., Tan, S.F., and Ross, F.M. (2023). Temperature dependent nanochemistry and growth kinetics using liquid cell transmission electron microscopy. *ACS Nano* **17**, 5609–5619. <https://doi.org/10.1021/acsnano.2c11477>.
23. Yang, Y., Shi, C., Feijóo, J., Jin, J., Chen, C., Han, Y., and Yang, P. (2024). Dynamic evolution of copper nanowires during CO₂ reduction probed by *operando* electrochemical 4D-STEM and X-ray spectroscopy. *J. Am. Chem. Soc.* **146**, 23398–23405. <https://doi.org/10.1021/jacs.4c06480>.
24. Mehdi, B.L., Qian, J., Nasybulin, E., Park, C., Welch, D.A., Faller, R., Mehta, H., Henderson, W.A., Xu, W., Wang, C.M., et al. (2015). Observation and quantification of nanoscale processes in lithium batteries by *operando* electrochemical (S)TEM. *Nano Lett.* **15**, 2168–2173. <https://doi.org/10.1021/acs.nanolett.5b00175>.
25. Hu, H., Li, J., Zhang, Q., Ding, G., Liu, J., Dong, Y., Zhao, K., Yu, M., Wang, H., and Cheng, F. (2023). Non-concentrated electrolyte with weak anion coordination enables low Li-ion desolvation energy for low-temperature lithium batteries. *Chem. Eng. J.* **457**, 141273. <https://doi.org/10.1016/j.cej.2023.141273>.
26. Chen, S., Chen, J., Liao, X., Li, Y., Wang, W., Huang, R., Zhao, T., Yan, S., Yan, Z., Cheng, F., and Wang, H. (2022). Enabling low-temperature and high-rate Zn metal batteries by activating Zn nucleation with single-atomic sites. *ACS Energy Lett.* **7**, 4028–4035. <https://doi.org/10.1021/acsenergylett.2c02042>.
27. Sacci, R.L., Black, J.M., Balke, N., Dudney, N.J., More, K.L., and Unocic, R.R. (2015). Nanoscale imaging of fundamental Li battery chemistry: Solid-electrolyte interphase formation and preferential growth of lithium metal nanoclusters. *Nano Lett.* **15**, 2011–2018. <https://doi.org/10.1021/nl5048626>.
28. Sacci, R.L., Dudney, N.J., More, K.L., Parent, L.R., Arslan, I., Browning, N.D., and Unocic, R.R. (2014). Direct visualization of initial SEI morphology and growth kinetics during lithium deposition by *in situ* electrochemical transmission electron microscopy. *Chem. Commun.* **50**, 2104–2107. <https://doi.org/10.1039/C3CC49029G>.
29. Leenheer, A.J., Jungjohann, K.L., Zavadil, K.R., Sullivan, J.P., and Harris, C.T. (2015). Lithium electrodeposition dynamics in aprotic electrolyte observed *in situ* via transmission electron microscopy. *ACS Nano* **9**, 4379–4389. <https://doi.org/10.1021/acsnano.5b00876>.
30. Dachraoui, W., Kühnel, R.-S., Battaglia, C., and Erni, R. (2024). Nucleation, growth and dissolution of Li metal dendrites and the formation of dead Li in Li-ion batteries investigated by *operando* electrochemical liquid cell scanning transmission electron microscopy. *Nano Energy* **130**, 110086. <https://doi.org/10.1016/j.nanoen.2024.110086>.
31. Zeng, H., Huang, R., Lin, J., Li, G., Jiang, Y., Liao, H.-G., and Sun, S.-G. (2023). Shape-controlled Zn nanosheet electrodeposition revealed by *in situ* liquid-phase transmission electron microscopy. *J. Phys. Chem. C* **127**, 22992–22999. <https://doi.org/10.1021/acs.jpcc.3c06164>.
32. Sasaki, Y., Yoshida, K., Kawasaki, T., Kuwabara, A., Ukyo, Y., and Ikuhara, Y. (2021). *In situ* electron microscopy analysis of electrochemical Zn deposition onto an electrode. *J. Power Sources* **481**, 228831. <https://doi.org/10.1016/j.jpowsour.2020.228831>.
33. Zhang, Q., Ma, J., Mei, L., Liu, J., Li, Z., Li, J., and Zeng, Z. (2022). *In situ* TEM visualization of LiF nanosheet formation on the cathode-electrolyte interphase (CEI) in liquid-electrolyte lithium-ion batteries. *Matter* **5**, 1235–1250. <https://doi.org/10.1016/j.matt.2022.01.015>.
34. Dachraoui, W., Pauer, R., Battaglia, C., and Erni, R. (2023). *Operando* electrochemical liquid cell scanning transmission electron microscopy investigation of the growth and evolution of the mosaic solid electrolyte interphase for lithium-ion batteries. *ACS Nano* **17**, 20434–20444. <https://doi.org/10.1021/acsnano.3c06879>.
35. Lee, D., Park, H., Ko, Y., Park, H., Hyeon, T., Kang, K., and Park, J. (2019). Direct observation of redox mediator-assisted solution-phase discharging of Li–O₂ battery by liquid-phase transmission electron microscopy. *J. Am. Chem. Soc.* **141**, 8047–8052. <https://doi.org/10.1021/jacs.9b02332>.
36. Seo, H.K., Hwa, Y., Chang, J.H., Park, J.Y., Lee, J.S., Park, J., Cairns, E.J., and Yuk, J.M. (2020). Direct visualization of lithium polysulfides and their suppression in liquid electrolyte. *Nano Lett.* **20**, 2080–2086. <https://doi.org/10.1021/acs.nanolett.0c00058>.
37. Arán-Ais, R.M., Rizo, R., Grosse, P., Algara-Siller, G., Dembélé, K., Plodinec, M., Lunkenbein, T., Chee, S.W., and Cuenya, B.R. (2020). Imaging electrochemically synthesized Cu₂O cubes and their morphological evolution under conditions relevant to CO₂ electroreduction. *Nat. Commun.* **11**, 3489. <https://doi.org/10.1038/s41467-020-17220-6>.
38. Gao, W., Hou, Y., Hood, Z.D., Wang, X., More, K., Wu, R., Xia, Y., Pan, X., and Chi, M. (2018). Direct *in situ* observation and analysis of the formation of palladium nanocrystals with high-index facets. *Nano Lett.* **18**, 7004–7013. <https://doi.org/10.1021/acs.nanolett.8b02953>.
39. Shi, F., Tieu, P., Hu, H., Peng, J., Zhang, W., Li, F., Tao, P., Song, C., Shang, W., Deng, T., et al. (2024). Direct *in-situ* imaging of electrochemical corrosion of Pd-Pt core-shell electrocatalysts. *Nat. Commun.* **15**, 5084. <https://doi.org/10.1038/s41467-024-49434-3>.
40. Beermann, V., Holtz, M.E., Padgett, E., de Araujo, J.F., Muller, D.A., and Strasser, P. (2019). Real-time imaging of activation and degradation of carbon supported octahedral Pt–Ni alloy fuel cell catalysts at the nanoscale using *in situ* electrochemical liquid cell STEM. *Energy Environ. Sci.* **12**, 2476–2485. <https://doi.org/10.1039/C9EE01185D>.
41. Lutz, L., Dachraoui, W., Demortière, A., Johnson, L.R., Bruce, P.G., Grimaud, A., and Tarascon, J.-M. (2018). *Operando* monitoring of the solution-mediated discharge and charge processes in a Na–O₂ battery using liquid-electrochemical transmission electron microscopy. *Nano Lett.* **18**, 1280–1289. <https://doi.org/10.1021/acs.nanolett.7b04937>.
42. Zhou, S., Shi, J., Liu, S., Li, G., Pei, F., Chen, Y., Deng, J., Zheng, Q., Li, J., Zhao, C., et al. (2023). Visualizing interfacial collective reaction behaviour of Li-S batteries. *Nature* **621**, 75–81. <https://doi.org/10.1038/s41586-023-06326-8>.
43. Nagashima, S., Ikai, T., Sasaki, Y., Kawasaki, T., Hatanaka, T., Kato, H., and Kishita, K. (2019). Atomic-level observation of electrochemical platinum dissolution and redeposition. *Nano Lett.* **19**, 7000–7005. <https://doi.org/10.1021/acs.nanolett.9b02382>.
44. Seo, H.K., Park, J.Y., Chang, J.H., Dae, K.S., Noh, M.-S., Kim, S.-S., Kang, C.-Y., Zhao, K., Kim, S., and Yuk, J.M. (2019). Strong stress-composition coupling in lithium alloy nanoparticles. *Nat. Commun.* **10**, 3428. <https://doi.org/10.1038/s41467-019-11361-z>.
45. Lee, S.-Y., Shangguan, J., Alvarado, J., Betzler, S., Harris, S.J., Doeff, M.M., and Zheng, H. (2020). Unveiling the mechanisms of lithium dendrite suppression by cationic polymer film induced solid–electrolyte interphase modification. *Energy Environ. Sci.* **13**, 1832–1842. <https://doi.org/10.1039/D0EE00518E>.
46. Zeng, Z., Barai, P., Lee, S.-Y., Yang, J., Zhang, X., Zheng, W., Liu, Y.-S., Bustillo, K.C., Ercius, P., Guo, J., et al. (2020). Electrode roughness dependent electrodeposition of sodium at the nanoscale. *Nano Energy* **72**, 104721. <https://doi.org/10.1016/j.nanoen.2020.104721>.
47. Balaghi, S.E., Mehrabani, S., Mousazade, Y., Bagheri, R., Sologubenko, A.S., Song, Z., Patzke, G.R., and Najafpour, M.M. (2021). Mechanistic understanding of water oxidation in the presence of a copper complex by *in situ* electrochemical liquid transmission electron microscopy. *ACS Appl. Mater. Interfaces* **13**, 19927–19937. <https://doi.org/10.1021/acsami.1c00243>.
48. Gong, C., Pu, S.D., Gao, X., Yang, S., Liu, J., Ning, Z., Rees, G.J., Capone, I., Pi, L., Liu, B., et al. (2021). Revealing the role of fluoride-rich battery electrode interphases by *operando* transmission electron microscopy. *Adv. Energy Mater.* **11**, 2003118. <https://doi.org/10.1002/aenm.202003118>.
49. Bhatia, A., Cretu, S., Hallot, M., Folastre, N., Berthe, M., Troadec, D., Roussel, P., Pereira-Ramos, J.-P., Baddour-Hadjean, R., Lethien, C.,

- and Demortière, A. (2022). In situ liquid electrochemical TEM investigation of $\text{LiMn}_{1.5}\text{Ni}_{0.5}\text{O}_4$ thin film cathode for micro-battery applications. *Small Methods* 6, 2100891. <https://doi.org/10.1002/smt.202100891>.
50. Fu, Q., Wong, L.W., Zheng, F., Zheng, X., Tsang, C.S., Lai, K.H., Shen, W., Ly, T.H., Deng, Q., and Zhao, J. (2023). Unraveling and leveraging in situ surface amorphization for enhanced hydrogen evolution reaction in alkaline media. *Nat. Commun.* 14, 6462. <https://doi.org/10.1038/s41467-023-42221-6>.
 51. Gong, C., Pu, S.D., Zhang, S., Yuan, Y., Ning, Z., Yang, S., Gao, X., Chau, C., Li, Z., Liu, J., et al. (2023). The role of an elastic interphase in suppressing gas evolution and promoting uniform electroplating in sodium metal anodes. *Energy Environ. Sci.* 16, 535–545. <https://doi.org/10.1039/D2EE02606F>.
 52. Hou, J., Song, Z., Odziomek, M., and Tarakina, N.V. (2023). Probing sodium storage mechanism in hollow carbon nanospheres using liquid phase transmission electron microscopy. *Small* 19, 2301415. <https://doi.org/10.1002/smll.202301415>.
 53. Yang, Y., Louisia, S., Yu, S., Jin, J., Roh, I., Chen, C., Fonseca Guzman, M.V., Feijóo, J., Chen, P.-C., Wang, H., et al. (2023). Operando studies reveal active Cu nanograins for CO_2 electroreduction. *Nature* 614, 262–269. <https://doi.org/10.1038/s41586-022-05540-0>.
 54. Tan, S.F., Roslie, H., Salim, T., Han, Z., Wu, D., Liang, C., Teo, L.F., and Lam, Y.M. (2024). Operando electrodeposition of nonprecious metal copper nanocatalysts on low-dimensional support materials for nitrate reduction reactions. *ACS Nano* 18, 19220–19231. <https://doi.org/10.1021/acsnano.4c04947>.
 55. Zhang, Q., Song, Z., Sun, X., Liu, Y., Wan, J., Betzler, S.B., Zheng, Q., Shangquan, J., Bustillo, K.C., Ercius, P., et al. (2024). Atomic dynamics of electrified solid-liquid interfaces in liquid-cell TEM. *Nature* 630, 643–647. <https://doi.org/10.1038/s41586-024-07479-w>.
 56. Liao, H.-G., Cui, L., Whitlam, S., and Zheng, H. (2012). Real-time imaging of Pt_3Fe nanorod growth in solution. *Science* 336, 1011–1014. <https://doi.org/10.1126/science.1219185>.
 57. Chen, L., Leonardi, A., Chen, J., Cao, M., Li, N., Su, D., Zhang, Q., Engel, M., and Ye, X. (2020). Imaging the kinetics of anisotropic dissolution of bimetallic core-shell nanocubes using graphene liquid cells. *Nat. Commun.* 11, 3041. <https://doi.org/10.1038/s41467-020-16645-3>.
 58. Yang, J., Zeng, Z., Kang, J., Betzler, S., Czarnik, C., Zhang, X., Ophus, C., Yu, C., Bustillo, K., Pan, M., et al. (2019). Formation of two-dimensional transition metal oxide nanosheets with nanoparticles as intermediates. *Nat. Mater.* 18, 970–976. <https://doi.org/10.1038/s41563-019-0415-3>.
 59. Park, J., Dutta, S., Sun, H., Jo, J., Karanth, P., Weber, D., Tavabi, A.H., Durmus, Y.E., Dzieciol, K., Jodat, E., et al. (2024). Toward quantitative electrodeposition via in situ liquid phase transmission electron microscopy: Studying electroplated zinc using basic image processing and 4D STEM. *Small Methods* 8, 2400081. <https://doi.org/10.1002/smt.202400081>.
 60. Merkens, S., Tollan, C., De Salvo, G., Bejtka, K., Fontana, M., Chiodoni, A., Kruse, J., Iriarte-Alonso, M.A., Grzelczak, M., Seifert, A., and Chuviilin, A. (2024). Toward sub-second solution exchange dynamics in flow reactors for liquid-phase transmission electron microscopy. *Nat. Commun.* 15, 2522. <https://doi.org/10.1038/s41467-024-46842-3>.
 61. Kim, J., Jones, M.R., Ou, Z., and Chen, Q. (2016). In situ electron microscopy imaging and quantitative structural modulation of nanoparticle superlattices. *ACS Nano* 10, 9801–9808. <https://doi.org/10.1021/acsnano.6b05270>.
 62. Hong, J., Bae, J.-H., Jo, H., Park, H.-Y., Lee, S., Hong, S.J., Chun, H., Cho, M.K., Kim, J., Kim, J., et al. (2022). Metastable hexagonal close-packed palladium hydride in liquid cell TEM. *Nature* 603, 631–636. <https://doi.org/10.1038/s41586-021-04391-5>.
 63. Schwager, P., Fenske, D., and Wittstock, G. (2015). Scanning electrochemical microscopy of oxygen permeation through air-electrodes in lithium-air batteries. *J. Electroanal. Chem.* 740, 82–87. <https://doi.org/10.1016/j.jelechem.2014.12.040>.
 64. Rong, G., Zhang, X., Zhao, W., Qiu, Y., Liu, M., Ye, F., Xu, Y., Chen, J., Hou, Y., Li, W., et al. (2017). Liquid-phase electrochemical scanning electron microscopy for in situ investigation of lithium dendrite growth and dissolution. *Adv. Mater.* 29, 1606187. <https://doi.org/10.1002/adma.201606187>.
 65. Tennyson, E.M., Gong, C., and Leite, M.S. (2017). Imaging energy harvesting and storage systems at the nanoscale. *ACS Energy Lett.* 2, 2761–2777. <https://doi.org/10.1021/acsenergylett.7b00944>.
 66. Zhang, Z., Said, S., Smith, K., Jervis, R., Howard, C.A., Shearing, P.R., Brett, D.J.L., and Miller, T.S. (2021). Characterizing batteries by in situ electrochemical atomic force microscopy: A critical review. *Adv. Energy Mater.* 11, 2101518. <https://doi.org/10.1002/aenm.202101518>.
 67. Pedraza-Tardajos, A., Claes, N., Wang, D., Sánchez-Iglesias, A., Nandi, P., Jenkinson, K., De Meyer, R., Liz-Marzán, L.M., and Bals, S. (2024). Direct visualization of ligands on gold nanoparticles in a liquid environment. *Nat. Chem.* 16, 1278–1285. <https://doi.org/10.1038/s41557-024-01574-1>.
 68. Abellan, P., Mehdi, B.L., Parent, L.R., Gu, M., Park, C., Xu, W., Zhang, Y., Arslan, I., Zhang, J.-G., Wang, C.-M., et al. (2014). Probing the degradation mechanisms in electrolyte solutions for Li-ion batteries by in situ transmission electron microscopy. *Nano Lett.* 14, 1293–1299. <https://doi.org/10.1021/nl404271k>.
 69. Grogan, J.M., Schneider, N.M., Ross, F.M., and Bau, H.H. (2014). Bubble formation in liquid induced by an electron beam. *Nano Lett.* 14, 359–364. <https://doi.org/10.1021/nl404169a>.
 70. Zhang, D., Zhu, Y., Liu, L., Ying, X., Hsiung, C.-E., Sougrat, R., Li, K., and Han, Y. (2018). Atomic-resolution transmission electron microscopy of electron beam-sensitive crystalline materials. *Science* 359, 675–679. <https://doi.org/10.1126/science.aao0865>.
 71. Wu, H., Friedrich, H., Patterson, J.P., Sommerdijk, N.A.J.M., and de Jonge, N. (2020). Liquid-phase electron microscopy for soft matter science and biology. *Adv. Mater.* 32, 2001582. <https://doi.org/10.1002/adma.202001582>.
 72. Zeng, Z., Zhang, X., Bustillo, K., Niu, K., Gammer, C., Xu, J., and Zheng, H. (2015). In situ study of lithiation and delithiation of MoS_2 nanosheets using electrochemical liquid cell transmission electron microscopy. *Nano Lett.* 15, 5214–5220. <https://doi.org/10.1021/acs.nanolett.5b02483>.
 73. Zeng, Z., Liang, W.-I., Liao, H.-G., Xin, H.L., Chu, Y.-H., and Zheng, H. (2014). Visualization of electrode-electrolyte interfaces in $\text{LiPF}_6/\text{EC}/\text{DEC}$ electrolyte for lithium ion batteries via in situ TEM. *Nano Lett.* 14, 1745–1750. <https://doi.org/10.1021/nl403922u>.
 74. Egerton, R.F. (2013). Control of radiation damage in the TEM. *Ultramicroscopy* 127, 100–108. <https://doi.org/10.1016/j.ultramic.2012.07.006>.
 75. Paillet, M., Wong, A., Denisov, S.A., Soudan, P., Poizot, P., Montigny, B., Mostafavi, M., Gauthier, M., and Le Caër, S. (2023). Predicting degradation mechanisms in lithium bistriflimide “water-in-salt” electrolytes for aqueous batteries. *ChemSusChem* 16, e202300692. <https://doi.org/10.1002/cssc.202300692>.
 76. Robertson, A.W., Zhu, G., Mehdi, B.L., Jacobs, R.M.J., De Yoreo, J., and Browning, N.D. (2018). Nanoparticle immobilization for controllable experiments in liquid-cell transmission electron microscopy. *ACS Appl. Mater. Interfaces* 10, 22801–22808. <https://doi.org/10.1021/acsmi.8b03688>.
 77. Tarnev, T., Cychy, S., Andronescu, C., Muhler, M., Schuhmann, W., and Chen, Y.-T. (2020). A universal nano-capillary based method of catalyst immobilization for liquid-cell transmission electron microscopy. *Angew. Chem. Int. Ed.* 59, 5586–5590. <https://doi.org/10.1002/anie.201916419>.
 78. Yang, R., Mei, L., Fan, Y., Zhang, Q., Liao, H.-G., Yang, J., Li, J., and Zeng, Z. (2023). Fabrication of liquid cell for in situ transmission electron microscopy of electrochemical processes. *Nat. Protoc.* 18, 555–578. <https://doi.org/10.1038/s41596-022-00762-y>.
 79. Stricker, E.A., Ke, X., Wainright, J.S., Unocic, R.R., and Savinell, R.F. (2019). Current density distribution in electrochemical cells with small cell heights and coplanar thin electrodes as used in EC-S/TEM cell

- geometries. *J. Electrochem. Soc.* *166*, H126–H134. <https://doi.org/10.1149/2.0211904jes>.
80. Zhang, X., Liu, W., Chen, Z., Huang, Y., Liu, W., and Yu, Y. (2022). Pitfalls in electrochemical liquid cell transmission electron microscopy for dendrite observation. *Adv. Energy Sustainability Res.* *3*, 2100160. <https://doi.org/10.1002/aesr.202100160>.
81. Gu, M., Parent, L.R., Mehdi, B.L., Unocic, R.R., McDowell, M.T., Sacci, R.L., Xu, W., Connell, J.G., Xu, P., Abellan, P., et al. (2013). Demonstration of an electrochemical liquid cell for operando transmission electron microscopy observation of the lithiation/delithiation behavior of Si nanowire battery anodes. *Nano Lett.* *13*, 6106–6112. <https://doi.org/10.1021/nl403402q>.
82. Kushima, A., So, K.P., Su, C., Bai, P., Kuriyama, N., Maebashi, T., Fujiwara, Y., Bazant, M.Z., and Li, J. (2017). Liquid cell transmission electron microscopy observation of lithium metal growth and dissolution: Root growth, dead lithium and lithium flotsams. *Nano Energy* *32*, 271–279. <https://doi.org/10.1016/j.nanoen.2016.12.001>.
83. Yin, S., Yi, H., Liu, M., Yang, J., Yang, S., Zhang, B.-W., Chen, L., Cheng, X., Huang, H., Huang, R., et al. (2024). An in situ exploration of how Fe/N/C oxygen reduction catalysts evolve during synthesis under pyrolytic conditions. *Nat. Commun.* *15*, 6229. <https://doi.org/10.1038/s41467-024-50629-x>.
84. Xie, Y., Wang, J., Savitzky, B.H., Chen, Z., Wang, Y., Betzler, S., Bustillo, K., Persson, K., Cui, Y., Wang, L.-W., et al. (2023). Spatially resolved structural order in low-temperature liquid electrolyte. *Sci. Adv.* *9*, eadc9721. <https://doi.org/10.1126/sciadv.adc9721>.
85. Yang, Y., Zhou, J., Zhao, Z., Sun, G., Moniri, S., Ophus, C., Yang, Y., Wei, Z., Yuan, Y., Zhu, C., et al. (2024). Atomic-scale identification of active sites of oxygen reduction nanocatalysts. *Nat. Catal.* *7*, 796–806. <https://doi.org/10.1038/s41929-024-01175-8>.
86. Smith, J., and Chen, Q. (2021). Enabling low-dose liquid-phase TEM with advanced signal processing, machine learning, and molecular simulation. *Microsc. Microanal.* *27*, 1314–1315. <https://doi.org/10.1017/S1431927621004906>.
87. Yao, L., Ou, Z., Luo, B., Xu, C., and Chen, Q. (2020). Machine learning to reveal nanoparticle dynamics from liquid-phase TEM videos. *ACS Cent. Sci.* *6*, 1421–1430. <https://doi.org/10.1021/acscentsci.0c00430>.
88. Vo, G., Zakharov, D., and Park, C. (2021). Data association algorithm for large-scale multi-object tracking with complex interactions. *J. Electron. Imaging* *30*, 063021. <https://doi.org/10.1117/1.JEI.30.6.063021>.
89. Chen, H., Qin, Z., He, M., Liu, Y., and Wu, Z. (2020). Application of electrochemical atomic force microscopy (EC-AFM) in the corrosion study of metallic materials. *Materials* *13*, 668. <https://doi.org/10.3390/ma13030668>.
90. Fan, G., Xu, W., Li, J., Chen, J.-L., Yu, M., Ni, Y., Zhu, S., Su, X.-C., and Cheng, F. (2021). Nanoporous nisb to enhance nitrogen electroreduction via tailoring competitive adsorption sites. *Adv. Mater.* *33*, 2101126. <https://doi.org/10.1002/adma.202101126>.